Carbon roadmap from syngas to polyhydroxyalkanoates in *Rhodospirillum rubrum*

Revelles O, Tarazona N, García JL and Prieto MA*

Department of Environmental Biology, Centro de Investigaciones Biológicas, Consejo Superior de Investigaciones Científicas (CSIC), 28040 Madrid, Spain.

*For correspondence. E-mail auxi@cib.csic.es; Tel. (+34) 918373112.

Keywords: *Rhodospirillum rubrum*, polyhydroxyalkanoates, syngas, CO metabolism, CO assimilation

*Corresponding author: M. Auxiliadora Prieto

Centro de Investigaciones Biológicas, CSIC

C/Ramiro de Maeztu, 9, 28040, Madrid, Spain

Running title: CO metabolism in *Rhodospirillum rubrum*

This article has been accepted for publication and undergone full peer review but has not been through the copyediting, typesetting, pagination and proofreading process, which may lead to differences between this version and the Version of Record. Please cite this article as doi: 10.1111/1462-2920.13087

Summary

The gasification of organic waste materials to synthesis gas (syngas), followed by microbial fermentation provides a significant resource for generating bioproducts such as polyhydroxyalkanoates (PHA). The anaerobic photosynthetic bacterium, *Rhodospirillum rubrum*, is an organism particularly attractive for the bioconversion of syngas into PHAs. In this study, a quantitative physiological analysis of *R. rubrum* was carried out by implementing GC-MS and HPLC techniques to unravel the metabolic pathway operating during syngas fermentation that leads to PHA production. Further, detailed investigations of the central carbon metabolites using ^{13}C-labeled substrate showed significant CO_2 assimilation (of 40 %) into cell material and PHA from syngas carbon fraction. By a combination of quantitative gene expression and enzyme activity analyses, the main role of carboxylases from the central carbon metabolism in CO_2 assimilation was shown, where the Calvin Benson-Bassham Cycle (CBB) played a minor role. This knowledge sheds light about the biochemical pathways that contribute to synthesis of PHA during syngas fermentation being valuable information to further optimize the fermentation process.

Introduction

Valorization and reuse of wastes through their bioconversion into value-added products is one of the most distinctive strategies of European Bio-economy. Organic waste provides a significant source of biomass that can be utilized for generating commodity products such as chemicals, biofuels or bioplastics (Munasinghe and Khanal, 2010; Latif *et al.*, 2014) by a bacterial fermentation process. Through gasification or pyrolysis, organic matter can be converted into a mixture of gases, composed mainly of CO, H_2 and CO_2 known as synthesis gas or syngas. Such gaseous mixture could be used by carbon-fixing microorganisms as carbon and energy sources and converted into high-added value products, in a process known as syngas fermentation. The feasibility to convert simple carbon precursors like CO_2 into a value-added product such as 3-hydroxybutyrate has been already reported (Wang Bo et al., 2013).

Syngas fermentation offers an attractive economic prospect for biofuel, fine chemicals and biopolymer production (Latif *et al.*, 2014; Beneroso *et al.*, 2015). Polyhydroxyalkanoates (PHAs) are one of the potential products that can be obtained from bioconversion of syngas via fermentation. *Rhodospirillum rubrum*, a purple non photosynthetic bacterium, is an organism particularly attractive for the bioconversion of syngas into PHAs and H_2 (Klasson *et al.*, 1993; Do *et al.*, 2007). PHAs are polyesters synthesized by many bacteria as an energy and carbon storage molecule (Liebergesell *et al.*, 1991; Verlinden *et al.*, 2007). These polymers are thermoplastics offering an alternative to oil-derived plastics since can be biodegraded by many microorganisms (Reddy *et al.*, 2003). Furthermore, the different monomers can be combined within this family giving a broad range of materials with different properties, what make these bioplastics suitable for several applications that range

from biomedical implants to packaging items. Polyhydroxybutyrate (PHB) is the most widely and best characterized PHA. PHB biosynthetic pathway consists of three enzymatic reactions catalyzed by three different enzymes. The first step is the condensation of two acetyl-CoA molecules into acetoacetylCoA by 3-ketothiolase (PhaA). Then, acetoacetyl-CoA reductase (PhaB) allows the reduction of acetoacetyl-CoA by NADH to 3-hydroxybutyryl-CoA. Lastly, the (*R*)-3-hydroxybutyryl-CoA monomers are polymerized into PHB by PHB synthase (PhaC). Often the genes that encoded these proteins are organized in a PHA biosynthetic operon that contains *phaA, phaB* and *phaC.* (Steinbüchel *et al.,* 1992).

One of the main challenges in the commercialization of syngas fermentation for the production of PHAs relies on its low productivity (Choi *et al.,* 2010). In order to overcome such limitation more information about the pathways and factors that affect syngas fermentation is needed. It has been suggested that *R. rubrum* can use CO under anaerobic conditions as carbon and energy source, having the highest specific CO uptake rate and conversion yield among different bacteria tested (Zhu *et al.,* 2001). When exposed to CO, both a CO-dehydrogenase (CODH) and a CO-insensitive hydrogenase are induced. The combined activities result in the biological oxidation of CO into CO_2 (Uffen, 1976; Kerby *et al.,*1995):

$$CO + H_2O \rightarrow CO_2 + 2H^+ + 2e^- \rightarrow CO_2 + H_2$$

R. rubrum can fix CO_2 into cell material through effective CO_2-fixing Calvin-Benson-Bassham (CBB) cycle. This cycle is under a tight regulation and very sensitive to environmental signals. The main role of the CBB cycle is to fix CO_2 into organic carbon under photoautotrophic conditions where CO_2 serves as the sole carbon source. However,

the CO_2 fixation metabolism depends on environmental metabolic variables (Slater and Morris, 1973). During photoautotrophic conditions the CBB cycle is mainly involved in CO_2 fixation, while on photoheterotrophic conditions this pathway plays an important role as a redox sink in the balance of reduction equivalents (McEwan, 1994). Potentially, in a photoheretrophic context other carboxylases beside ribulose 1,5 biphosphate carboxylase/oxygenase (Rubisco) could catalyze the direct transformation of inorganic carbon into central precursor molecules (Figure 1) (Erb *et al.,* 2012). Although there is no experimental evidence so far, the CO_2 released from the CODH activity can potentially be assimilated into organic substrate by assimilatory reactions that involve other carboxylases (Figure 1).

The main objective of the present research work was to study the metabolic capability of *R. rubrum* to ferment syngas under different conditions directed towards PHAs production, as well as, to demonstrate CO assimilation into biomass. In order to prove the assimilation of CO into biomass, different experimental procedures were carried out. By ^{13}C analysis and gene expression analysis was shown that others carboxylases than Rubisco are actively incorporating CO_2 from syngas into biomass. Additionally, our results show the main role of acetate providing the carbon skeleton for PHAs and biomass synthesis. The role of CODH in the redox potential and ATP synthesis is further discussed in this paper.

Results

Nutrient requirements of *R. rubrum* for growing in syngas.

R. rubrum is able to oxidize CO to CO_2 and H_2O to H_2 (Figure 1) (Uffen, 1976). However, previous studies stressed that *R. rubrum* requires traces of other carbon sources such as acetate and yeast extract to growth on syngas (Zhu *et al.*, 2001; Younesi et al., 2008). The RRNCO media (*R. rubrum* no-light carbon monoxide, containing yeast extract (YE) and acetate, see experimental procedures) (Kerby *et al*., 1995) was used as initial reference for syngas fermentation studies. First at all, to demonstrate that *R. rubrum* can use syngas to grow, the cells were cultivated anaerobically into 20 mL of RRNCO medium in a 100 mL serum bottle either in darkness or in the presence of light. These cultures were supplemented daily with 80 ml of syngas at 1 atm. A high ratio of gas volume to liquid volume and vigorous stirring of the cell suspension were supplied to enhance gas-liquid mass transfer phase throughout the growth period. In parallel control cultures on RRNCO medium without syngas were carried in both conditions: light and darkness. A growth rate (μ) of 0.07 h^{-1} was achieved in the culture with syngas, both in light and in darkness, as well as in the control culture without syngas but in the presence of light (Figure 2). No growth was detected in the absence of syngas in darkness. These data indicate that the carbon fraction (*i.e*, acetate and YE) from RRNCO medium cannot support alone the growth in darkness, suggesting that syngas is needed at least as energy source in absence of light. In order to get more insight into the physiology of *R. rubrum* and CO metabolism, the effects of acetate and YE during syngas fermentation were assessed. The cell growth in darkness with SYN medium containing 1 gL^{-1} YE and different acetate concentrations (0 to 10 mM) was monitored for 120 h where syngas was added daily (Table 1). The inclusion of acetate accelerated the cell growth significantly by a factor of four. Interestingly the accumulation of PHA is tightly related to acetate concentration. Finally, removing YE from the medium but keeping a concentration of 10 mM of acetate decreased the growth rate

four times while the percentage of PHA accumulation was not affected. Under the conditions tested a co-polymer composed of approximately 99% hydroxybutyrate and 1% hydroxyvalerate was identified at the end of the exponential phase of growth.

These results suggest that YE is not essential for syngas fermentation but acetate is required for PHA production and growth under the conditions studied (Figure_2SD). In this sense, acetate as well as other non-fermentable organic substrates, such as malate, require energy from the electron transport-linked phosphorylation to support anaerobic respiration growth (Schultz and Weaver, 1982). Previous findings provided direct evidence that the CO-to-H_2 pathway is linked to ATP production (Maness et *al.*, 2005), and these results suggested that syngas fermentation will provide the energy that cells require to grow with acetate in darkness, however, there was still no evidence that CO or CO_2 were assimilated into the biomass or PHA in these growth conditions.

The effect of non-fermentable organic acids and light conditions in the growth kinetic and PHB production on syngas.

Najafpour and Younesi (2007) showed that a limited light intensity has a positive effect on the efficiency of growth and CO conversion to H_2 and CO_2, however nothing has been reported regarding its effect on PHA yield. Our results proved that YE is not essential for *R. rubrum* when growing in syngas, but an alternative carbon source like acetate is needed to grow and efficiently synthesize PHA (Table 1). To further investigate the syngas assimilation and PHA production in *R. rubrum*, different parameters were investigated such as carbon source requirements and light *versus* darkness conditions. With this aim the SYN

146 medium, defined above, was used as the basal medium for the following experiments (see
147 Experimental Procedures).
148 The effect of light on biomass and PHA yield is showed in Table 2 comparatively when
149 using two different non-fermentable organic acids, acetate or malate. Two parallel cultures
150 were grown in serum bottle in SYN medium plus 10 mM acetate in darkness and in light.
151 Light slightly accelerated the μ (h^{-1}) from 0.021 to 0.029 and increased of the biomass
152 production yield from acetate ($gDWg^{-1}$), from 1.4 to 1.5. The acetate uptake rate
153 ($mmol.g.DW^{-1}h^{-1}$) was almost not affected by the effect of light during syngas
154 fermentation. The presence of extracellular by-products was measured by HPLC, and none
155 intermediate was detected. Furthermore, regarding PHA accumulation, it was not detected
156 any remarkable change in its productivity indicating that the photosynthetic apparatus does
157 not affect PHA production/accumulation under the tested conditions.
158 *R. rubrum* grew on malate at a higher rate (0.058 h^{-1}) to that observed on acetate (0.021 h^{-1}). Interestingly, a higher concentration of malate is needed in darkness (2.58 $mmol.g.DW^{-1}.h^{-1}$) to achieve the same rate of growth than in light (1.07 $mmol.g.DW^{-1}.h^{-1}$), suggesting
161 that cells are growing with different metabolic efficiencies. The biomass production yield
162 from malate was the same in light (1.30 $gDW.g^{-1}$) and in darkness (1.33 $gDW.g^{-1}$). Along
163 the growth curve, malate was converted into acetate that was secreted as a by-product to the
164 extracellular medium to be further co-consumed with malate at the mid-end exponential
165 phase. Interestingly almost not PHA accumulation was detected in the presence of malate.
166 The CO and CO_2 consumption along the growth curve was monitored on cells growing in
167 acetate in light or in darkness. A sample (1 mL) from the head-space of the culture bottle
168 (see Experimental Procedures) was taken at time zero (after adding syngas to the culture)

and after 48 h (in light) or 72 h (in darkness) of incubation. The differences in the final gas composition were measured using a gas chromatograph (GC) equipped with a thermal conductivity detector (TCD). Values acquired from this experiment are shown in Table 3. The cells growing in syngas-acetate medium in light showed around 50% of CO and CO_2 conversion from the initial concentration on syngas, while in darkness the CO and CO_2 conversion was about 40%. Our data clearly show a consumption of CO and CO_2 from syngas in both conditions, with an uptake of 1.5-fold and 1.2-fold higher of CO and CO_2 in light than in darkness, respectively.

Identification and gene expression profile of potential routes involved in CO assimilation and PHB production from syngas and acetate

In order to get a comprehensive view of CO assimilation into biomass, an expression analysis of genes potentially involved in the assimilation/fixation of CO_2 was carried out. A preliminary identification based on the literature (see below), genome annotation and KEGG (Kyoto Encyclopedia of Genes and Genome) pathway database analysis was performed to identify potential assimilatory reactions that involve CO_2 fixation into organic compounds in *R. rubrum*.

It has been stressed above that in a photoheretrophic context other carboxylases besides Rubisco might catalyze CO_2 assimilation. Our study suggests that acetate assimilation in *R. rubrum* could be possible *via* three different routes that involve carboxylation and therefore CO_2 incorporation to central metabolites (Buchanan and Evans, 1965; Buchanan et al., 1967; Berg and Ivanovsky, 2009; Hadicke *et al.*, 2011). These pathways and their carboxylases are compiled in Figure 1. One of these routes involves the ferredoxin-

dependent pyruvate synthase (PFOR) enzyme coded by the *Rru_A2398* gene, following the reversible reaction:

$$\text{Acetyl-CoA} + \text{NADPH} + CO_2 \leftrightarrow \text{Pyruvate} + \text{CoA} + NADP^+$$

Another alternative route for acetate assimilation is the ethylmalonyl-CoA (EMCoA) pathway. The crotonyl-CoA reductase (Ccr) coded by the *Rru_A3063* gene catalyzes the carboxylation of crotonyl-CoA in the reversible reaction:

$$\text{Crotonyl-CoA} + CO_2 + \text{NADH} \leftrightarrow \text{EMCoA} + \text{NAD}.$$

The citramalate (CM) cycle has been also proposed for acetate assimilation (Berg and Ivanovsky, 2009). CM and EMCoA share the propionyl-CoA carboxylation reaction, catalyzed by the propionyl-CoA carboxylase yielding methylmalonyl-CoA (MEMACoA) coded by the *Rru_A1943* gene in the reaction:

$$\text{Propionyl-CoA} + \text{ATP} + CO_2 \leftrightarrow \text{MEMACoA} + \text{ADP} + \text{Pi} + H^+$$

The expression of the Rubisco encoding gene (*Rru_A1998*) was also analyzed because Anderson and Fuller (1967) have reported high expression levels in phototrophically-grown cells, but it is also active under photoheterotrophic conditions.

The last enzyme involved in CO_2 carboxylation reactions considered in this study was the *o*-oxoglutarate synthase encoded by the *Rru_A2721* gene that has been also identified in *R. rubrum* (Buchanan *et al.*, 1967).

Finally, the transcriptional regulator CooA encoded by the *Rru_A1431* gene that regulates the expression of genes involved in CO oxidation and that is induced by CO (Roberts *et al.*, 2005) was included in the expression profile analyses.

The expression levels of all these genes were monitored by qRT-PCR in cells grown in different conditions: a) syngas plus acetate in light *versus* syngas plus acetate in darkness

(Table 4;[a]FC), b); syngas plus acetate *versus* syngas plus malate both in darkness (Table 4;[b]FC) and c) and syngas plus acetate *versus* malate both in darkness (Table 4;[c]FC).

When light and darkness conditions were compared in the presence of acetate, the expression level of *cooA* showed no variation (Table 4 [a]FC). This observation suggests that there are not differences in the regulation of CO metabolism during syngas fermentation regarding light or darkness. However, Rubisco showed an expression 3-fold higher in cells growing in light than in darkness (see Discussion). The expression levels of the other genes coding for crotonyl-CoA reductase, pyruvate synthase, 2-oxoglutarate synthase and PEP carboxykinase, were upregulated in light about 2-fold, 3-fold, 10-fold and 3-fold, respectively.

Furthermore, when the expression levels of these genes were compared between cells grown in darkness with syngas in two different carbon sources, acetate and malate (Table 4 [b]FC), the expression of *Rru_A3063* (crotonyl-CoA reductase) and *Rru_A2398* (pyruvate synthase) was 6-fold higher in the presence of acetate, as expected because these enzymes are involved in acetate assimilation (see reactions above).

The expression levels of *cooA* in cells grown in syngas-acetate in darkness were 25-fold higher than those in cells grown in syngas-malate on darkness, indicating that *cooA* is upregulated in syngas-acetate compared to syngas-malate.

Finally, the expression levels of all these genes were determined in cells grown in syngas plus acetate and compared with those of cells grown in malate both on darkness (Table 4;[c]FC). The expression levels of *cooA* were 65-fold higher in cells grown in syngas-acetate than in cells grown in malate, indicating a strong upregulation of *cooA* by syngas. Regarding the genes encoding the carboxylases, crotonyl-CoA reductase and pyruvate synthase, the highest expression levels were found in cells grown in acetate, confirming the

role of the enzymes in acetate assimilation. For the others carboxylases (propionyl-CoA carboxylase-*Rru_A1943* and 2-oxoglutarate synthase-*Rru_A2721*), no differences in the level of transcripts were found in cells grown in these conditions (Table 4 ^{b}FC and ^{c}FC), suggesting that the activity of such carboxylases is independent of syngas and the carbon source present on the culture medium.

Finally, the expression of the genes involved in the PHA pathway was also monitored. Previous studies and genome sequencing have revealed that *R. rubrum* can express three different PHA polymerases *phaC1*, *phaC2* and *phaC3* coded by *Rru_A0275*, *Rru_A2413* and *Rru_A1816* genes, respectively, being *phaC2* the most relevant gene for PHA production (Hustede *et al.*, 1992; Jin and Nikolau, 2012). Further, *phaC1* is located adjoining the *phaA* (*Rru_A0274*) and *phaB* (*Rru_A0273*) homologous genes in the PHA biosynthetic operon. Upstream there is a potential regulator, *phaR* (*Rru_A0276*). The expression levels of all these genes were determined and compared in cells grown in darkness with syngas plus acetate, and cells grown in darkness with malate. Surprisingly, there were no significant differences in the expression of these genes in both conditions at mid-exponential phase (Table 4 ^{c}FC), suggesting that the expression of PHA biosynthetic operon at exponential phase of growth is not a limiting step for PHA production.

Metabolic profile of *R. rubrum* during syngas fermentation

Taken together the results presented above pointed out the role of syngas as energy source but did not demonstrate its role as carbon source, *i.e.*, the active assimilation of CO into biomass. Moreover, the transcriptomic data suggested a putative role of pyruvate synthase (Rru_A2398), crotonyl-CoA carboxylase (Rru_A3063) and Rubisco (Rru_A1998) in

syngas assimilation. To ascertain this hypothesis, a ^{13}C-isotopomer-based target metabolome analysis was carried out in order to determine if CO is converted into biomass. *R. rubrum* was cultivated in SYN media containing syngas and [U-^{13}C]-acetate. Then, an extensive number of metabolites derived from cell cultivation during syngas fermentation in darkness and in light were examined. The sole source of ^{12}C came exclusively from the carbon fraction of syngas (^{12}CO and $^{12}CO_2$). To better understand the metabolites flow in *R. rubrum*, the incorporation of ^{13}C atoms into the above mentioned metabolites was evaluated by mean of ^{13}C-MID (mass isotopomer distribution) analysis (Figure 3). Figure S1 shows the ^{13}C enrichment of each metabolite calculated from experimental MIDs. The patterns of incorporation of labeled carbon atoms in phosphoenolpyruvic acid (PEP) has been used to provide information about the carboxylation reaction catalyzed by pyruvate synthase, since the metabolites pyruvate (Pyr) and PEP share the same ^{13}C-labeled carbon skeletons. Pyr had only two ^{13}C atoms of three carbons that come directly from [U-^{13}C]-acetate, the other carbon can be only associated with CO_2 fixation. The ^{13}C-mass isotopomer labeling pattern of PEP (M0, M1, M2 and M3) revealed a 20% of one unlabeled carbon ^{12}C (M2) in its carbon skeletons that will be derived from the above mentioned reaction, and therefore, a direct evidence of ^{12}C incorporation from syngas, both in darkness and in light. The same label pattern was found for the metabolite 1,3 biphosphoglycerate (1,3-BPG).

R. rubrum can in principle assimilate CO_2 through the CBB cycle. If CBB were actively assimilating CO_2 into biomass in our growth conditions, the pattern of incorporation of unlabeled carbon in the 3-phosphoglycerate (3-PG) metabolite would be higher, and therefore a dilution in the ^{13}C enrichment would be expected. 2-PG (2-phosphoglycerate) isomer could be also formed *via* glycolysis/gluconeogenesis. However, isomer pairs 2/3-PG

285 could not be differentiated because they co-eluted and had identical m/z, so they are
286 referred as 2/3 PG. Interestingly no differences regarding the ^{13}C-mass isotopomer labeling
287 pattern and ^{13}C-enrichment between PEP and 2/3-PG metabolite were found, indicating an
288 undetectable contribution of CBB cycle to CO_2 assimilation between the two conditions
289 tested. Same results were observed for the metabolite sedoheptulose-7P (S7P) of the
290 pentose phosphate pathway (PPP) (Figure 3). These findings are in agreement with
291 previous observation under photoherotrophic conditions in the presence of organic carbon,
292 such as acetate, that suggested that the CBB cycle is involved in the maintenance of the
293 redox balance in the cell, but not in CO_2 fixation (McKinlay and Harwood, 2010 ; 2011;
294 Gordon and McKinlay, 2014).

295 Concerning the analysis of EMCoA pathway, it is important to stress than in this study the
296 CoA intermediates were not identified due to incompatibility of technical protocols. Thus,
297 the activity of this route was determined indirectly by detecting the ^{13}C-enrichment in TCA
298 metabolites such as α-ketoglutarate and citrate. The results shown in Figure_1SD
299 demonstrate 20% of ^{13}C-enrichment as an average.

300 Finally, we measured the labeling profile of PHB by analyzing hydroxybutyrate mass
301 isotopomer using GC-MS (see experimental procedures) and comparing with the natural
302 abundance of each isotopomer. The results indicated a slightly higher unlabeled carbon in
303 the isotope m/z 130 in light than in darkness (Table 5). Furthermore, around 20-30% of one
304 unlabeled carbon in this isotope was found in both conditions, showing a similar pattern to
305 that found for carbon central metabolites.

306

307 **Carboxylation activities in cell extracts of *R. rubrum* during syngas fermentation.**

The upregulation in the expression level of the genes that codify carboxylases (Ccr and PFOR) and the ^{13}C-MID analysis were strongly indicating ^{12}C assimilation from syngas into metabolite as a result of metabolic carboxylases activity. To validate these results, two main carboxylases, ferredoxin-dependent pyruvate synthase (PFOR) and crotonyl-CoA carboxylase/reductase (Ccr), were selected based on their role in the acetate metabolism. The enzyme activities were further analyzed in crude extracts of cells grown in syngas with acetate 10 mM, both in light and in darkness. PFOR catalyses the reverse carboxylation of acetyl-CoA to generate pyruvate and the rate of the reaction depends exclusively on the concentration of acetyl-CoA and pyruvate. PFOR activity is expected to be stimulated in the presence of acetate in the cultures (Leroy *et al.*, 2015). A control experiment was performed with cells growing in the presence of acetate 30 mM showing that this step is functional in these growth conditions (Figure 4, panel A). Therefore, when the bacteria are growing in syngas and acetate the net flux through this enzyme favors the pyruvate synthesis. The direction of this flux is supported in this study by ^{13}C-mass isotopomer labeling pattern of PEP (see above) and the upregulation of *Rru_A2398*. Besides, Figure 4 shows that, the PFOR is functional in the crude extracts of cells grown on syngas with 10 mM of acetate in darkness or in light (8 ± 2 and 15 ± 5, respectively) fully demonstrating its role in CO_2 assimilation from syngas in these growth conditions.

Leroy and coworkers (2015) have shown the role of EMC pathway in acetate assimilation, where the Ccr exhibited a high activity level in acetate (see control experiment panel B, Figure 4). In agreement with the increment of *Rru_A3063* (Ccr) expression level detected during syngas fermentation in acetate (Table 4), a Ccr specific activity of 18 and 25, in

darkness and light respectively were detected (Figure 4, panel B), demonstrating an active CO_2 assimilation at this metabolic network level.

Summing up, the carboxylases from the central carbon metabolism are actively assimilating carbon from syngas. Whether this carbon fraction comes mainly from CO oxidation or from the CO_2 present in syngas will need further demonstration, but the variation on the gases concentration from syngas in the uptake experiments demonstrated that CO is consumed by *R. rubrum.*

Discussion

R. rubrum is one of the scarce bacteria able to grow in syngas while producing PHAs. A CODH and a CO-insensitive hydrogenase, both associated to the chromatophore membranes, are induced by CO catalyzing the oxidation of CO to CO_2. However, carbon assimilation from CO to biomass or PHA had never been confirmed. The first conclusion derived from this study is that syngas cannot be used as single carbon source in this bacterium, evidencing the need of an additional carbon source to support growth. Acetate and malate have been tested as non-fermentable acids to improve biomass formation (malate or acetate) and final PHA production (exclusively with acetate). These carbon sources have been chosen because they need light or an alternative source of reducing equivalents to obtain energy for supporting the growth on anaerobic conditions, since there is no ATP synthesis via substrate-level phosphorylation in their dissimilation. Thus, on photoheterotrophic conditions, *R. rubrum* obtains energy from light and carbon from the organic compounds, *e.g.*, acetate or malate. However, in darkness another source of energy is required. Our results demonstrate that *R. rubrum* can effectively use CO as energy source

353 being essential to propagate in darkness. This is in agreement with previous observations,
354 suggesting that CO oxidation and subsequent reduction of protons for H_2 production, could
355 be coupled to the generation of a proton motive force and the synthesis of ATP (Ensign and
356 Ludden, 1991; Fox *et al.*, 1996; Maness *et al.*, 2005). Further, although *R. rubrum* growth
357 is not light dependent, the light has a slight positive effect in the biomass yield, growth rate
358 and specific uptake rate. The beneficial effect of light is reflected both at physiological
359 level and at metabolic level, suggested by the high levels of transcripts found in this
360 condition, i.e., transcripts of crotonyl-CoA reductase, pyruvate synthase, 2-oxoglutarate
361 synthase and PEP-carboxykinase are induced more than twice in light compared to
362 darkness. Further, the specific activities of Ccr and PFOR were higher in light than in
363 darkness, 1-fold and 0.5-fold higher, respectively. This is in agreement with the observation
364 made by Najafpour and Younesi (2007) who pointed out the positive effect of light
365 intensity in *R. rubrum* during syngas fermentation.
366 Although it is known that *R. rubrum* uses CO as energy source generating CO_2, the fixation
367 of the carbon fraction (CO and CO_2) from syngas had never been analyzed. Thus, an
368 important conclusion of this work is that CO can be assimilated via CO_2 into biomass and
369 PHA in the presence of acetate. The assimilation of $^{12}CO_2$ from syngas is revealed by mean
370 of ^{13}C-labelling experiments. The analysis of ^{13}C-mass isotopomer labeling pattern of
371 carbon central metabolites and PHA showed that about 40% of the metabolite pool has ^{12}C
372 in its carbon backbone. This result is also supported by the concomitant consume of CO
373 and CO_2 registered (~50 %), indicating that all the CO converted into CO_2 was consumed
374 by the cells. These data are a clear indication that CO metabolism is actively channeling
375 CO into CO_2, and it is finally assimilated as biomass and PHA. Further, the expression of
376 CO metabolism was confirmed by quantifying the transcription levels of its key regulator

CooA. The CO-sensing transcription activator CooA is responsible of the expression of the multicomponent CO oxidation system. A high level of *cooA* transcript was found in syngas cultures regardless the condition tested, demonstrating its role in CO uptake, since this regulator is specifically induced by CO (Roberts *et al.*, 2005). Unexpectedly, when acetate was used as co-substrate, a higher level of *cooA* transcript (25-fold) was found. Taking into account that acetate cannot be used as energy source, this result suggests that acetate stimulates the CO uptake to obtain the energy required for growth and for PHA biosynthesis.

In order to improve PHA production, the roadmap of carbon from the C1 fraction of syngas and acetate must be drawn. Therefore, the assimilatory reactions potentially involved in CO/CO_2 fixation into organic substrates have been assessed, when the culture was fed with acetate as co-substrate. Two alternative pathways have been proposed for acetate assimilation in *R. rubrum* (Figure 1) including two carboxylases; crotonly-CoA reductase (Rru_A3063) and pyruvate synthase (Rru_A2398). The high level of transcript, *i.e.*,6-fold higher than in malate found for the genes encoding these carboxylases suggest that they are acting in the $^{12}CO_2$ assimilation. Further, the carboxylase activities of these enzymes have been verified in crude extracts of cells growing in syngas supplemented with acetate. These data provide information on these enzymes as potential targets to optimize strains by metabolic engineering strategies. In addition, these carboxylases could play multiple functions being involved not only in acetate assimilation but also fixing the C1 fraction of syngas. The genes encoding the others carboxylases tested in this study (propionyl-CoA carboxylase-Rru_A1943 and 2-oxoglutarate synthase-Rru_A2721) showed no differences in the level of transcript in darkness either in malate or acetate with or without syngas

(Table 4 ^{b}FC and ^{c}FC). These data suggest that the expression of these carboxylases is constitutive in the conditions tested, being independent of syngas and the carbon source present on the medium.

McKinlay and Harwood (2010; 2011) showed the important role of CBB cycle on photoheterotrophic conditions to maintain the internal redox balance when the carbon source used to grow is more oxidized than biomass, as it is the case of acetate. During syngas fermentation, either in light or in darkness, no differences in the label pattern of the 2/3 PG pool was detected indicating an almost undetectable CBB flux. These results suggest that during syngas fermentation CO metabolism could be responsible of maintaining redox balance, most probably through the CO-insensitive hydrogenases, and therefore, CBB cycle is playing a minor role in carbon assimilation. On the other hand, it is worth to mention that beside the undetectable CBB cycle flux identified, a high level of Rubisco expression has been measured in light, being 3-fold higher in light than in darkness. However, the lack of correlation between the gene enzyme expression levels and the metabolic flux observed here has been often described elsewhere (Glanemann *et al.*, 2003; Siddiquee *et al.*, 2004; Nanchen *et al.*, 2008).

Syngas fermentation is currently raising a great interest in the production of value-added chemicals that justify the efforts addressed to metabolically engineer microorganisms for improving the production yields (Griffin and Schultz, 2012). Although there are many approaches to convert syngas into biofuels like ethanol, the use of syngas as substrate to produce biopolymers has been rarely explored (Do *et al.,* 2007). This research sheds light on the metabolic network of syngas fermentation providing potentials targets to metabolically engineer *R. rubrum* in order to increase PHA production.

Experimental procedures

Cultivation conditions.

Starter cultures of *R. rubrum* (ATCC 11170) were grown under anaerobic conditions on RRNCO medium (Kerby *et al.*, 1995) supplemented with 15 mM fructose at 30ºC until stationary phase (OD_{600} 1.5). Briefly, RRNCO medium contains per liter of distilled water: 2 µg of biotin, 10 mL of a chelated iron-molybdenum solution (0.28 g of H_3BO_3, 2 g of Na_2EDTA, 0.4 g of ferric citrate, and 0.1 g of Na_2MoO_4 per liter of distilled water), 250 mg of $MgSO_4$ $7H_2O$, 132 mg of $CaCl_2$ $2H_2O$, 1 g of NH_4Cl, 20 µM $NiCl_2$, 1.0 g of yeast extract, 2.1 g of MOPS and 0.82 g of sodium acetate. Prior inoculation, anoxic solutions of 1.91 M potassium phosphate (pH 7.0) (0.05 mL), of 1% Na_2S $9H_2O$ (0.1 mL) and of 0.5 M $NaHCO_3$ (pH 8.0) (0.25 mL) were added. This culture was used as preinoculum for syngas fermentation. Syngas experiments were done in a RRNCO modified medium named SYN where yeast extract and acetate were removed. SYN medium was supplied with 10 mM acetate or 5 mM malate when indicated. Syngas fermentation was carried out in bottles of 100 mL containing 20 mL of SYN medium. Prior adding syngas the closed degasified serum vials were subjected to 1 min vacuum-purge and the atmosphere were further saturated with syngas to 1 atm of pressure. This procedure was repeated every day for syngas feeding. Syngas composition is made out of 40% CO, 40% H_2, 10% CO_2 and 10% N_2 (Air Liquide, www.airliquide.com). The source of light was supplied by a compact fluorescent lamp (Ralux Long RX-L 36W/840/2G11) to the serum bottles at 1000 lux when indicated. For ^{13}C-labelling experiments, acetate was replaced by 10 mM 99% [U-^{13}C]-acetate (Cambridge Isotope Laboratories, Inc). The inoculum was adjusted to an initial OD_{600} of 0.05 from the preculture described above, and was harvest at OD_{600} 0.5. Further,

447 Inoculation was performed after centrifugation and washing with the same medium
448 deprived of carbon source.
449
450 Growth characterization.
451 The growth rate (μ) was determined from log-linear regression of time-dependent changes
452 in optical density at 600 nm (OD_{600}), measured with a spectrophotometer (UV-VIS
453 Spectrophotometer Shimatzu UV mini 1240) with appropriate dilutions when needed.
454 Acetate and malate were quantified using an HPLC system (GILSON), equipped with an
455 Aminex HPX-87H column. A mobile phase of 2.5 mM H_2SO_4 solution at a 0.6 $mLmin^{-1}$
456 flow rate was used and the column was operated at 40ºC. Rates of disappearance and/or
457 appearance of substrates and products in the culture supernatants were determined
458 (Revelles *et al.*, 2013). To calculate specific biomass yields, correlation factors between
459 cell dry weights and optical density (g_{CDW}/OD_{600}) were established for each condition.
460
461 Real-time qRT-PCR assays.
462 Cultures were harvested at 4ºC at mid-exponential phase and frozen immediately at -80ºC.
463 RNA purification was carried out using High Pure RNA isolation Kit (Roche) as specified
464 by the manufacturer. Extracted RNA was treated with RNasefree (Ambion) following
465 manufacturer's instructions. RNA integrity was checked by agarose gel electrophoresis. The
466 absence of contaminating DNA was analyzed by real time PCR using primers for 16S
467 rRNA as described below. Gene expressions analyses were performed by a two-step RT-
468 qPCR approach using SYBR Green I dye in a LightCycler 480 II Roche®. In this two-step
469 RT-qPCR, the reverse transcription and PCR amplification steps were performed in two
470 separate reactions. First, cDNA was synthesized from 1 μg of purified RNA in random

hexamer primed reactions with the Transcriptor First Strand cDNA Synthesis Kit (Roche). After retrotranscription, PCR reactions were carried out in 96-well plates in a final volume of 20 µL containing: 100 ng of transcribed cDNA, 1 µM of each forward and reverse primer and 10 µL of SYBR Green Master Mix (FastStart Taq DNA Polymerasa, reaction buffer, dNTP mix, SYBER Green I dye and 8 mM $MgCl_2$). Cycling was performed as follows: pre-incubation at 95ºC for 10 min followed by 45 cycles of 5 s at 95ºC, 10 s at 60 ºC and 10 s at 72 ºC. After thermocycling, a melting curve was made to verity the specificity of the amplified PCR product. The sequence of the primers used for this study is listed in Table S1. The analysis was performed in three technical replicates from three biological samples. The results were analyzed using the $2^{-\Delta\Delta CT}$ method (Livak and Schmittgen, 2001) with a reference gene identified in this work. Fold change is expressed as a range, which is a result of incorporating the standard deviation of the $\Delta\Delta C_T$ value into the fold change calculation,

To determine a suitable reference gene, 6 candidate genes were assessed under different growth conditions to evaluate their stability. The evaluated genes were: 16S ribosomal RNA (*Rru_A0064*), glyceraldehyde-3-phosphate dehydrogenase (*Rru_A0222*), 23S ribosomal RNA (*Rru_A0043*), DNA gyrase subunit A (*Rru_A1744*), RNA polymerase sigma factor (*Rru_A2882*) and RNA polymerase subunit beta (*Rru_A2695*). RNA was isolated from cells grown at mid-exponential phase on three different carbon sources (30 mM acetate, 15 mM malate or 10 mM fructose) and two different conditions (darkness or light), and gene expression stability was analyzed by qRT-PCR. The expression stability for the reference genes was determined by statistical analysis using Statgraphics Centurion version XV software. Statistical significance level was set at p= 0.05. The results provided

16S rRNA as the most suitable reference gene. The primers used for this study are listed in the Table S1.

Cell extract and enzyme activity measurement.

Cells from mid-exponential cultures growing in syngas with 10 mM acetate in light or darkness were harvested, and resuspended in 50 mM Tris/HCl buffer (pH 7.9). After ultrasonic treatment for 3 min at 4ºC, unbroken organisms and cell debris were removed by centrifuging at 14 000 x *g* for 10 min at 4ºC. The resulting supernatant (crude extract) was used in enzymatic assays. The protein concentration was measured using the Bradford method (Bradford 1976), with bovine gamma-globulin as standard.

The crotonyl-CoA-dependent oxidation of NADPH was followed spectrophotometrically at 360 nm (ε_{NADPH}= 3,400 $M^{-1}cm^{-1}$) as described previously elsewhere (Erb *et al*., 2007). Briefly, the reaction mixture (0.5 ml) contained 100 mM Tris-HCl buffer (pH 7.9), 4 mM NADPH, 2 mM crotonyl-CoA, and 33 mM $NaHCO_3$. The reaction was started by the addition of 0.8 mg/ml of cell extract. Negative control was performed in the absence of crude extract and in the absence of co-factor and/or substrate.

Pyruvate synthase dependent oxidation was measured as describe previously (Furdui *et al*., 2000). The reaction mixture contained 10 mM pyruvate, 1 mM CoA, 1 mM thiamin pyrophosphate, 2 mM $MgCl_2$, 0.1 mM metronidazole and 1 µM ferredoxin in 50 mM Tris-HCl buffer (pH 7.9). The reaction was started by adding 0.8 mg/ml of cell extract, and the reduction of metronidazole was followed at 320 nm (ε_{320}= 9 300 $M^{-1}cm^{-1}$). Negative control was performed in the absence of crude extract and in the absence of co-factor and/or substrate.

Positive control was carried out on crude extracts from cells in mid-exponential phase that were grown in SYN medium supplemented with 30 mM acetate.

PHB/PHA quantification by GC analysis.

PHB/PHA was isolated and purified using cells harvested from different growing phases by centrifugation at 8 000 x *g* for 15 min at 4ºC (Eppendorf Centrifuge 5810R). Cells were then washed twice in distilled water and lyophilized in Cryodos-50 (Telstar, Terrasa, Spain) at -56ºC and 10^{-2} mbar. Further, PHB monomer composition and cellular PHB content were determined by gas chromatography (GC) of the methanolysed polyester. Methanolysis was carried out by suspending 5–10 mg of lyophilized cells in 0.5 mL of chloroform and 2 mL of methanol containing 15% sulfuric acid and 0.5 mg mL^{-1} of 3-methylbenzoic acid (internal standard), followed by an incubation at 80 °C for 7 h. After cooling, 1 mL of demineralized water and 1 mL of chloroform were added. The organic phase containing the methyl esters was analyzed by GC (de Eugenio *et al.*, 2010). A standard curve from 0.5 to 2 mg of PHB (Sigma Cat: 36,350-2) was used to interpolate sample data.

Sampling of intracellular metabolites for ^{13}C-metabolic analysis.

Sampling was performed at the mid-exponential phase (OD_{600} ~ 0.5) in two steps; i) rapid quenching of metabolism followed by ii) metabolite extraction. For quenching, 2 mL of broth were rapidly sprayed into precooled centrifuge tubes maintained at -80 °C and containing 5 mL of cold ethanol, homogenized using a vortex and centrifuged (12 000 x *g* for 5 min at -20 °C) with Eppendorf Centrifuge 5810R. Metabolites were extracted by pouring 5 mL of an ethanol/water (75/25) solution at 95 °C onto the cell pellets. After

incubation for 2 min in closed tubes, the cellular extracts were cooled on ice and stored at -80 °C. For each biological replicate, three metabolite samples were collected and analyzed.

Preparation of cellular extracts and IC-MS(/MS) analysis of intracellular metabolites.

Cellular extracts were evaporated for 4 h (SC110A SpeedVac Plus, ThermoSavant, USA). The remaining aqueous extracts were freeze-dried, resuspended in 200 µL of milliQ water and stored at -80 °C. Intracellular metabolites were analyzed as previously described (Revelles *et al.*, 2013). Briefly, analysis was performed by high performance anion exchange chromatography (Dionex ICS 2000 system, Sunnyvale, USA) coupled to a triple quadrupole QTrap 4000 (AB Sciex, CA) mass spectrometer. All samples were analyzed in the negative mode by multiple reaction monitoring (MRM). The injection volume was 15 µL, originating from approximately 2 µg of biomass. The ^{13}C-labeling patterns of central metabolites, including organic acids (Mal, Cit, Suc, α-KG) and phosphorylated compounds (G6P, F6P, FBP, PEP, 6PG, R5P, S7P, combined pools of 2-PG and 3-PG) were determined as described in (Bolten *et al.*, 2007; Revelles *et al.*, 2013). The labeling patterns (isotopologue distributions) were calculated from the isotopic clusters after correction for naturally occurring isotopes with IsoCor (Millard *et al.*, 2012). For the analysis of the ^{13}C-labell pattern of hydroxybutyrate (HB) the protocol already described above was followed. The isotopologue distribution of HB was calculated by monitoring the ion sets *m/z* 103-106.

Gas analysis.

The gases H_2, CO, and CO_2 were analyzed by using a gas chromatograph (Agilent 7890A GC) equipped with a thermal conductivity detector (TCD) and two columns connected in

series (80/100 Porapak Q and 70/80 Molesieve 13X). The initial oven temperature was 30 ºC, which was maintained with an isothermic step of 5 min. It was then programmed with a rate of 25 ºC min^{-1} until reached 180 ºC. The injector and detector temperatures were 150 and 250 ºC, respectively. Helium (Air Liquide, www.airliquide.com) was used as carrier gas. Samples were taken from the headspace of the culture at different times using a tight gas syringe and added to HS-vials, previously degasified with helium. Prior to the measurements the gas analyzer was calibrated by a standard gas and a calibration curve was established. The calculation for gas concentration was carried out using the GC data analysis software (ChemStation rev. B.04.03-SP1; Agilent Technologies, Inc.).

Acknowledgments

This work has been funded by the EU project SYNPOL (grant agreement n° 311815) under the European Union's Seventh Framework Programme. Natalia Tarazona is a PhD student granted by the Department of Science Technology and Innovation-Colciencias, Colombia. We thank MetaToul (Toulouse metabolomics & fluxomics facilities, www.metatoul.fr) for the excellent technical assistance. The technical support of Inmaculada Calvillo and Ana Valencia is very much appreciated.

Tables:

Table 1. Kinetic Growth parameters of *R. rubrum* with syngas in darkness under different growth conditions.

	ACETATE[a]			ACETATE[b]
SYNGAS				**(10 mM)**
DARKNESS	**0 mM**	**5 mM**	**10 mM**	**YE (0 gL^{-1})**
μ (h^{-1})	0.016±0.004	0.070±0.015	0.08±0.01	0.021±0.005
Qs ($mmol.gDW^{-1}.h^{-1}$)	ND	5.00±0.60	5.07±0.06	1.43±0.05
$Y_{x/s}$ ($gDW.g^{-1}$)	ND	1.30±0.15	1.30±0.10	1.45±0.50
PHA (% CDW)	2.7±0.8	12.0±1.0	20.0±15.0	28.0±10.0

Values represent the mean ± standard deviation of three independent biological replicates. μ (h^{-1}), specific growth rate; Qs ($mmol.gDW^{-1}.h^{-1}$), carbon source uptake rate; $Y_{x/s}$ ($gDW^{-1}.g^{-1}$), biomass production yield; PHA (% cell dry weight).

[a]A concentration of 1 gL^{-1} of yeast extract has been added to the medium, while different concentrations of acetate has been tested.

[b]All trace of yeast extract has been removed and fix concentration of 10 mM acetate has been used.

Table 2. Kinetic Growth parameters of *R. rubrum* with acetate and malate as co-substrates during syngas fermentation in darkness and in light.

SYNGAS	ACETATE (10 mM)		MALATE (5 mM)	
	LIGHT	DARKNESS	LIGHT	DARKNESS
μ (h^{-1})	0.029±0.005	0.021±0.005	0.058±0.005	0.058±0.005
Qs(mmol.$gDW^{-1}.h^{-1}$)	1.51±0.05	1.43±0.05	1.07±0.05	2.58±0.50
$Y_{x/s}$ ($gDW.g^{-1}$)	1.54±0.30	1.45±0.50	1.30±0.10	1.33±0.05
PHA (% CDW)	20.0±5.0	28.0±10.0	<1	<1

Values represent the mean ± standard deviation of three independent biological replicates. μ (h^{-1}), specific growth rate; Qs (mmol.$gDW^{-1}.h^{-1}$), carbon source uptake rate; $Y_{x/s}$ ($gDW^{-1}.g^{-1}$), biomass production yield; PHA (% cell dry weight).

Table 3. Gases consumption during syngas fermentation. The CO and CO_2 consumptions along the growth curve (48 h light and 72 h darkness) were determined. The differences in the final gas composition are given as percentage or mmoles of gas consumed.

GASES IN	LIGHT		DARKNESS		BLANK
SYNGAS	[a]%	[b]mmoles	[a]%	[b]mmoles	[a]%
CO 40%	53.00±0.40	0.60±0.01	37.00±1.00	0.43±0.04	5.00±2.00
CO_2 10%	50.00±0.10	0.12±0.01	41.00±0.50	0.10±0.01	2.00±0.50

[a]Percentage of gas conversion (%) from the initial concentration on syngas, and [b]mmoles consumed at the end of the growth. Values represent the mean ± standard deviation of three independent biological replicates.

603 **Table 4. Genes differentially expressed in *R. rubrum* under different syngas growth**
604 **conditions.**

Gene name	[a]FC	[b]FC	[c]FC	Description	Role in *R. rubrum*
Rru_A1431 (*cooA*)	0.5	25	65	Crp/Fnr family transcriptional regulator	Induce a multicomponent CO oxidation system
Rru_A1998	3	0.5	0.5	Ribulose 1,5-biphosphate carboxylase	CO_2 fixation
Rru_A3063	2	6	10	Crotonyl-CoA reductase	Methylmalonyl pathway
Rru_A2398	3	6	2	Pyruvate Synthase	Incomplete Reductive TCA Cycle
Rru_A1943	1	0.5	1.5	Propionyl CoA carboxylase	Methylmalonyl pathway
Rru_A2721	10	0.1	0.5	2-Oxoglutarate synthase	TCA cycle
Rru_A3419	3	1	1	PEP carboxykinase	Carbon metabolism
Rru_A2413 (*phaC2*)	ND	ND	0.5	Poly(R)-hydroxyalkanoic acid synthase	PHA metabolism
Rru_A0275	ND	ND	1	Poly(R)-	PHA metabolism

(*phaC1*)				hydroxyalkanoic acid synthase	
Rru_A1816 (*phaC3*)	ND	ND	0.5	Poly(R)-hydroxyalkanoic acid synthase, class I	PHA metabolism
Rru_A0274	ND	ND	0.5	Acetyl-CoA acetyltransferase	PHA metabolism
Rru_A0273	ND	ND	0.5	3-Oxoacyl-ACP reductase	PHA metabolism
Rru_A0276 (*phaR*)	ND	ND	1	PHB synthesis repressor PhaR	PHA metabolism

The results were corrected using 16S rRNA as housekeeping gene. The mean of three biological replicas and the standard deviation are shown.

[a]FC=Fold change- indicates up or downregulated in SYNGAS-Acetate light relative to SYNGAS-Acetate darkness.

[b]FC=Fold change- indicates up or downregulated in SYNGAS-Acetate relative to SYNGAS-Malate both in darkness.

[c]FC=Fold change- indicates up or downregulated in SYNGAS-Acetate relative to SYN-Malate both in darkness.

Table 5. Mass isotopomer distributions analysis of poly-hydroxybutyrate extracted from *R. rubrum* grown on syngas with 10 mM [U-^{13}C]-acetate in darkness and in light.

	MASS ISOTOPOMER DISTRIBUTION (MID)		
m/z 103	**DARKNESS**	**LIGHT**	**[a]NATURAL ABUNDANCE**
M0	0.03 ± 0.02	0.09 ± 0.03	0.950 ± 0.005
M1	0.14 ± 0.01	0.14 ± 0.01	0.040 ± 0.002
M2	0.21 ± 0.05	0.31 ± 0.05	0.010 ± 0.005
M3	0.62 ± 0.05	0.46 ± 0.01	0.000

The fragment ion used to identify and quantify hydroxybutyrate was the dominant *m/z* 103. M0 to M3 represent the m + 0 to m + 6 enrichments in ^{13}C. Data are shown as means ± s.d. of three independent experiments. [a]Natural abundance of the isotope 103 from experimental values of a pure standard compounds.

Figures legends

Figure 1. Metabolic network topology of the central carbon metabolism of *R. rubrum* on acetate during syngas fermentation. The two suggested pathways for acetate degradation on *R. rubrum* are highlighted in orange: Citramalate cycle (CM) and ethylmalonyl-CoA (EMCoA). The TCA cycle is highlighted in blue, the CO metabolism in grey, PHB cycle in green and CBB cycle and PPP in pink. The different carboxylases involved in CO_2 assimilation studied in this work are compiled in this figure as well as their corresponding genes. Further, the genes *Rru_A0274*, *Rru_A0273*, *Rru_A0275*, *Rru_A2413* and *Rru_A1816* implicated in PHB metabolism and also investigated in this study are shown in this figure. Abbreviations: 3PG, 3-phosphoglycerate; PEP, phosphoenolpyruvate; Pyr, pyruvate; AcCoA, acetyl coenzyme A; AcAcCoA, acetoacetyl coenzyme A; αKG, α-ketoglutarate; Cit/Icit, citrate/isocitrate; SuccCoA, succinyl-CoA; Suc, succinate; Mal, malate; OAA, oxalacetate; F6P, fructose 6-phosphate; G6P, glucose 6-phosphate; G3P, glyceraldehyde 3-phosphate; S7P, sedoheptulosa 7-phosphate; E4P, erythrose 4-phosphate; R5P, pentoses phosphates; R1,5P, ribulose 1,5-bisphosphate; 1,3-BPG, 1,3-bisphosphoglycerate; 3-HBCoA, 3-hydroxybutyrylCoA; PHB, polyhydroxybutyrate; EMCoA, ethylmalonyl coenzyme A; MEMACoA, methylmalonyl coenzyme A. The genes studied in this paper are highlighted in red.

Figure 2. *R. rubrum* growing on syngas. A) Anaerobic culture of *R. rubrum* on SYN medium plus 10 mM acetate in darkness. The bottle on the left side was supplemented with syngas while the bottle on the right side was not. B) A TEM (transmission electron microscopy) image of *R. rubrum* with granules of PHB.

Figure 3. Mass isotopomer distribution analyses of metabolites extracted from *R. rubrum* grown on syngas with 10 mM [U-^{13}C] acetate in darkness (coloured in black) and light (coloured in grey). M0 to M7 represent the m + 0 to m + 7 enrichments of stable isotope ^{13}C. A dilution in the m enrichment is given by the assimilation of ^{12}C from $^{12}CO_2$. Cells were incubated with [U-^{13}C] acetate and metabolites were extracted at mid exponential phase (OD_{600} 0.5). In all experiments, data are the average ± s.d. of three independent cultures.

Figure 4. Pyruvate synthase -PFOR (A) and crotonyl-CoA reductase/carboxylase-Ccr (B) activities. Crude extracts of *R. rubrum* grown with 30 mM acetate (positive control) or on Syngas with 10 mM acetate in light or in darkness were tested for pyruvate synthase-PFOR (A) and crotonyl-CoA reductase/carboxylase-Ccr activity (B).

References

1. Anderson, L., and Fuller, R.C. (1967) Photosynthesis in *Rhodospirillum rubrum*. II. Photoheterotrophic carbon dioxide fixation. *Plant Physiol* **42**: 491-496.
2. Beneroso, D., Bermúdez, J.M., Arenillas, A., and Menéndez, J.A. (2015) Comparing the composition of the synthesis-gas obtained from the pyrolysis of different organic residues for a potential use in the synthesis of bioplastics. *J Anal Appl Pyrol* **111**: 55-63.
3. Berg, I.A., and Ivanovsky, R.N. (2009) Enzymes of the citramalate cycle in *Rhodospirillum rubrum*. *Microbiology* **78**: 16-24.
4. Bradford M.M. (1976) A rapid and sensitive method for the quantitation of microgram quantities of protein utilizing the principle of protein-dye binding. *Anal Biochem* **72**: 248-254.
5. Bolten, C.J., Kiefer, P., Letisse, F., Portais, J.C., and Wittmann, C. (2007) Sampling for metabolome analysis of microorganisms. *Anal Chem* **79**: 3843-3849.
6. Buchanan, B.B., and Evans, M.C. (1965) The synthesis of alpha-ketoglutarate from succinate and carbon dioxide by a subcellular preparation of a photosynthetic bacterium. *Proc Natl Acad Sci USA* **54**: 1212-1218.
7. Buchanan, B.B., Evans, M.C., and Arnon, D.I. (1967) Ferredoxin-dependent carbon assimilation in *Rhodospirillum rubrum. Arch Mikrobiol* **59**: 32-40.
8. Choi, D., Chipman, D.C., Bents, S.C., and Brown, R.C. (2010) A techno-economic analysis of polyhydroxyalkanoate and hydrogen production from syngas fermentation of gasified biomass. *Appl Biochem Biotechnol* **160**: 1032-1046.
9. de Eugenio, L.I., Galán, B., Escapa, I.F., Maestro, B., Sanz, J.M., García, J.L., and Prieto, M.A. (2010) The PhaD regulator controls the simultaneous expression of the

pha genes involved in polyhydroxyalkanoate metabolism and turnover in *Pseudomonas putida* KT2442. *Environ Microbiol* **12**: 1591-1603.

10. Do, Y.S., Smeenk, J., Broer, K.M., Kisting, C.J., Brown, R., Heindel, T.J. *et al.* (2007) Growth of *Rhodospirillum rubrum* on synthesis gas: conversion of CO to H2 and poly-beta-hydroxyalkanoate. *Biotechnol Bioeng* **97**: 279-286.
11. Ensign, S.A., and Ludden, P.W. (1991) Characterization of the CO oxidation/H2 evolution system of *Rhodospirillum rubrum*. Role of a 22-kDa iron-sulfur protein in mediating electron transfer between carbon monoxide dehydrogenase and hydrogenase. *J Biol Chem* **266**: 18395-18403.
12. Erb, T.J., Berg, I.A., Brecht, V., Müller, M., Fuchs G. and Alber, B.E. (2007) Synthesis of C5-dicarboxylic acids from C2-units involving crotonyl-CoA carboxylase/reductase: the ethylmalonyl-CoA pathway. *Proc Natl Acad Sic USA.* **104:** 10631-6.
13. Erb, T.J., Evans, B.S., Cho, K., Warlick, B.P., Sriram, J., Wood, B.M. *et al.* (2012) A RubisCO-like protein links SAM metabolism with isoprenoid biosynthesis. *Nat Chem Biol* **8**: 926-932.
14. Fox, J.D., He, Y., Shelver, D., Roberts, G.P., and Ludden, P.W. (1996) Characterization of the region encoding the CO-induced hydrogenase of *Rhodospirillum rubrum*. *J Bacteriol* **178**: 6200-6208.
15. Furdui, C., and Ragsdale, S.W. (2000) The role of pyruvate ferredoxin oxidoreductase in pyruvate synthesis during autotrophic growth by the Wood-Ljungdahl pathway. *J Biol Chem* **275**: 28494-28499.
16. Glanemann, C., Loos, A., Gorret, N., Willis, L.B., O'Brien, X.M., Lessard, P.A. and Sinskey, A.J. (2003) Disparity between changes in mRNA abundance and enzyme

activity in *Corynebacterium glutamicum*: implications for DNA microarray analysis. *Appl Microbiol Biotechnol* **61**: 61-68.

17. Gordon, G.C., and McKinlay, J.B. (2014) Calvin cycle mutants of photoheterotrophic purple nonsulfur bacteria fail to grow due to an electron imbalance rather than toxic metabolite accumulation. *J Bacteriol* **196**: 1231-1237.
18. Griffin, D.W., and Schultz, M.A. (2012) Fuel and chemical products from biomass syngas: A comparison of gas fermentation to thermochemical conversion routes. *Environ Prog Sustainable Energy* **31**: 219-224.
19. Hädicke, O., Grammel, H., and Klamt, S. (2011) Metabolic network modeling of redox balancing and biohydrogen production in purple nonsulfur bacteria. *BMC Syst Biol* **5**: 150.
20. Hustede, E., Steinbüchel, A., and Schlegel, H.G. (1992) Cloning of poly(3-hydroxybutyric acid) synthase genes of *Rhodobacter sphaeroides* and *Rhodospirillum rubrum* and heterologous expression in *Alcaligenes eutrophus*. *FEMS Microbiol Lett* **72**: 285-290.
21. Jin, H., and Nikolau, B.J. (2012) Role of genetic redundancy in polyhydroxyalkanoate (PHA) polymerases in PHA biosynthesis in *Rhodospirillum rubrum*. *J Bacteriol* **194**: 5522-5529.
22. Kerby, R.L., Ludden, P.W., and Roberts, G.P. (1995) Carbon monoxide-dependent growth of *Rhodospirillum rubrum*. *J Bacteriol* **177**: 2241-2244.
23. Klasson, K.T., Gupta, A., Clausen, E.C., and Gaddy, J.L. (1993) Evaluation of mass-transfer and kinetic parameters for *Rhodospirillum rubrum* in a continuous stirred tank reactor. *Appl Biochem Biotechnol* **39-40**: 549-557.

24. Latif, H., Zeidan, A.A., Nielsen, A.T., and Zengler, K. (2014) Trash to treasure: production of biofuels and commodity chemicals via syngas fermenting microorganisms. *Curr Opin Biotechnol* **27**: 79-87.
25. Leroy, B., De Meur, Q., Moulin, C., Wegria, G. and Wattiez, R. (2015) New insight into the photoheterotrophic growth of the isocytrate lyase-lacking purple bacterium *Rhodospirillum rubrum* on acetate. *Microbiology* **161**: 1061-72
26. Liebergesell, M., Hustede, E., Timm, A., Steinbüchel, A., Fuller, R.C., Lenz, R.W, and Schlegel, H.G. (1991) Formation of poly(3-hydroxyalkanoates) by phototrophic and chemolithotrophic bacteria. *Arch Microbiol* **155**: 415-421.
27. Livak, K.J., and Schmittgen, T.D. (2001) Analysis of relative gene expression data using real-time quantitative PCR and the 2(-Delta Delta C(T)) method. *Methods* **25**: 402-408.
28. Maness, P.C., Huang, J., Smolinski, S., Tek, V., and Vanzin, G. (2005) Energy generation from the CO oxidation-hydrogen production pathway in *Rubrivivax gelatinosus*. *Appl Environ Microbiol* **71**: 2870-2874.
29. McEwan, A.G. (1994) Photosynthetic electron transport and anaerobic metabolism in purple non-sulfur phototrophic bacteria. *Anton Leeuw Int J G* 66: 151-164.
30. McKinlay, J.B., and Harwood, C.S. (2010) Carbon dioxide fixation as a central redox cofactor recycling mechanism in bacteria. *Proc Natl Acad Sci* 107: 11669-11675.
31. McKinlay, J.B., and Harwood, C.S. (2011) Calvin cycle flux, pathway constraints, and substrate oxidation state together determine the H2 biofuel yield in photoheterotrophic bacteria. *MBio* 2. doi:10.1128/mBio00323–10.

32. Millard, P., Letisse, F., Sokol, S., and Portais, J.C. (2012) IsoCor: correcting MS data in isotope labeling experiments. *Bioinformatics* 28: 1294-1296.
33. Munasinghe, P.C., and Khanal, S.K. (2010) Biomass-derived syngas fermentation into biofuels: Opportunities and challenges. *Bioresour Technol* 101: 5013-5022.
34. Najafpour, G.D., and Younesi, H. (2007) Bioconversion of synthesis gas to hydrogen using a light-dependent photosynthetic bacterium, *Rhodospirillum rubrum*. *World J Microbiol Biotechnol* **23**: 275-284.
35. Nanchen, A., Schicker, A., Revelles, O., and Sauer, U. (2008) Cyclic AMP-dependent catabolite repression is the dominant control mechanism of metabolic fluxes under glucose limitation in *Escherichia coli*. *J Bacteriol* **190**: 2323-2330.
36. Reddy, C.S., Ghai, R., Rashmi, and Kalia, V.C. (2003) Polyhydroxyalkanoates: an overview. *Bioresour Technol* **87**: 137-146.
37. Revelles, O., Millard, P., Nougayrède, J.P., Dobrindt, U., Oswald, E., Létisse, F., and Portais, J.C. (2013) The carbon storage regulator (Csr) system exerts a nutrient-specific control over central metabolism in *Escherichia coli* strain Nissle 1917. *PLoS One* **8**: e66386.
38. Roberts, G.P., Kerby, R.L., Youn, H., and Conrad, M. (2005) CooA, a paradigm for gas sensing regulatory proteins. *J Inorg Biochem* **99**: 280-292.
39. Schultz, J.E., and Weaver, P.F. (1982) Fermentation and anaerobic respiration by *Rhodospirillum rubrum* and *Rhodopseudomonas capsulata*. *J Bacteriol* **149**: 181-190.
40. Siddiquee, K.A.Z., Arauzo-Bravo, M.J., and Shimizu, K. (2004) Effect of a pyruvate kinase (*pykF*-gene) knockout mutation on the control of gene expression and metabolic fluxes in *Escherichia coli*. *FEMS Microbiol Letters* **235**: 25-33.

41. Slater, J.H., and Morris, I. (1973) The pathway of carbon dioxide assimilation in Rhodospirillum rubrum grown in turbidostat continuous-flow culture. *Arch Mikrobiol* **92**: 235-244.
42. Steinbüchel, A., Hustede, E., Liebergesell, M., Pieper, U., Timm, A., and Valentin, H. (1992) Molecular basis for biosynthesis and accumulation of polyhydroxyalkanoic acids in bacteria. *FEMS Microbiol Rev* **9**: 217–230.
43. Uffen, R.L. (1976) Anaerobic growth of a Rhodopseudomonas species in the dark with carbon monoxide as sole carbon and energy substrate. *Proc Natl Acad Sci USA* **73**: 3298-3302.
44. Verlinden, R.A., Hill, D.J., Kenward, M.A., Williams, C.D., and Radecka, I. (2007) Bacterial synthesis of biodegradable polyhydroxyalkanoates. *J Appl Microbiol* **102**: 1437-1449.
45. Wang, B., Pugh, S., Nielsen, D.R., Zhang, W., and Meldrum, D.R. (2013) Engineering cyanobacteria for photosynthetic production of 3-hydroxybutyrate from CO2. *Metab Eng* **16**: 68-77.
46. Younesi, H., Najafpour, G., Ku Ismail, KS., Mohamed, AR., and Kamaruddin, AH. (2008) Biohydrogen production in a continuous stirred tank bioreactor from synthesis gas by anaerobic photosynthetic bacterium: *Rhodospirillum rubrum*. *Bioresource Technol* **99**: 2612-2619.
47. Zhu, H., Wakayama, T., Asada, Y., and Miyake, J. (2001) Hydrogen production by four cultures with participation by anoxygenic photo-synthetic bacterium and anaerobic bacterium in the presence of NH4+. *Int J Hydrogen Energy* **26**: 1149-1154.

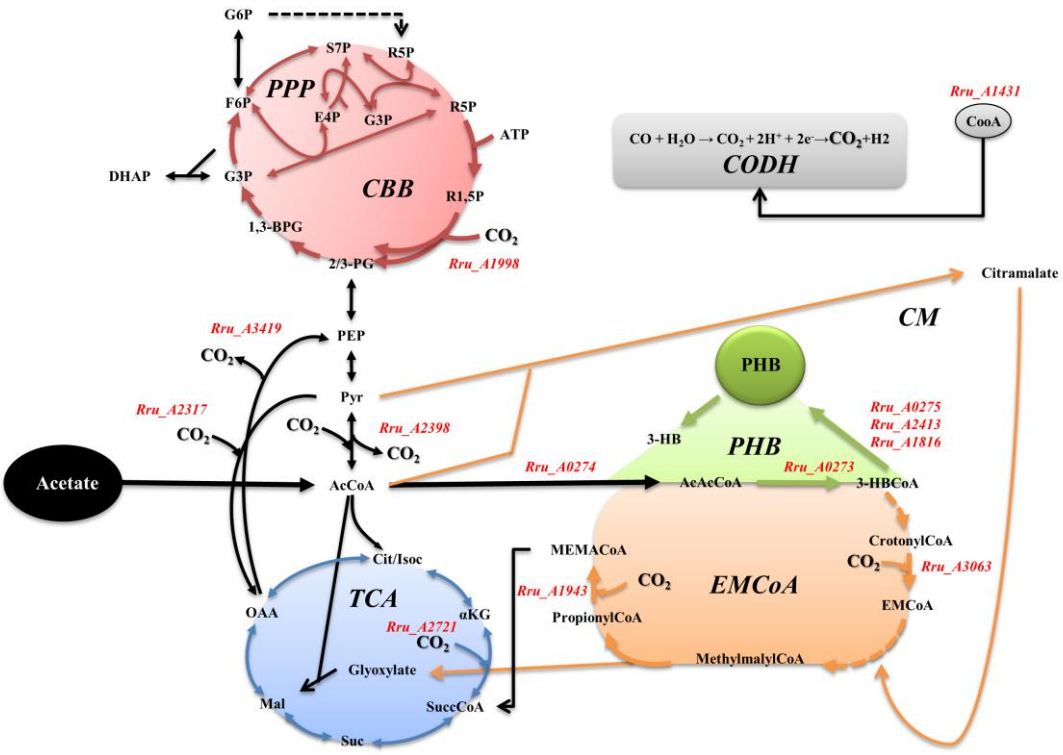

795

796 EMI_13087_F1

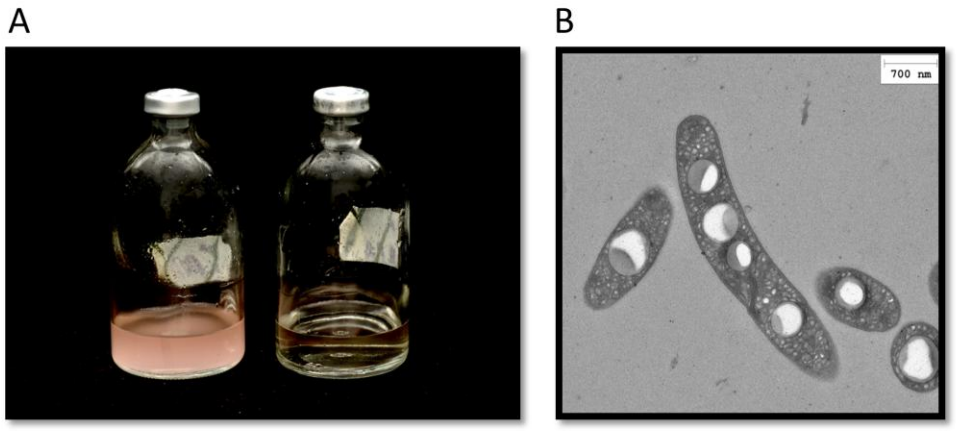

797

798 EMI_13087_F2

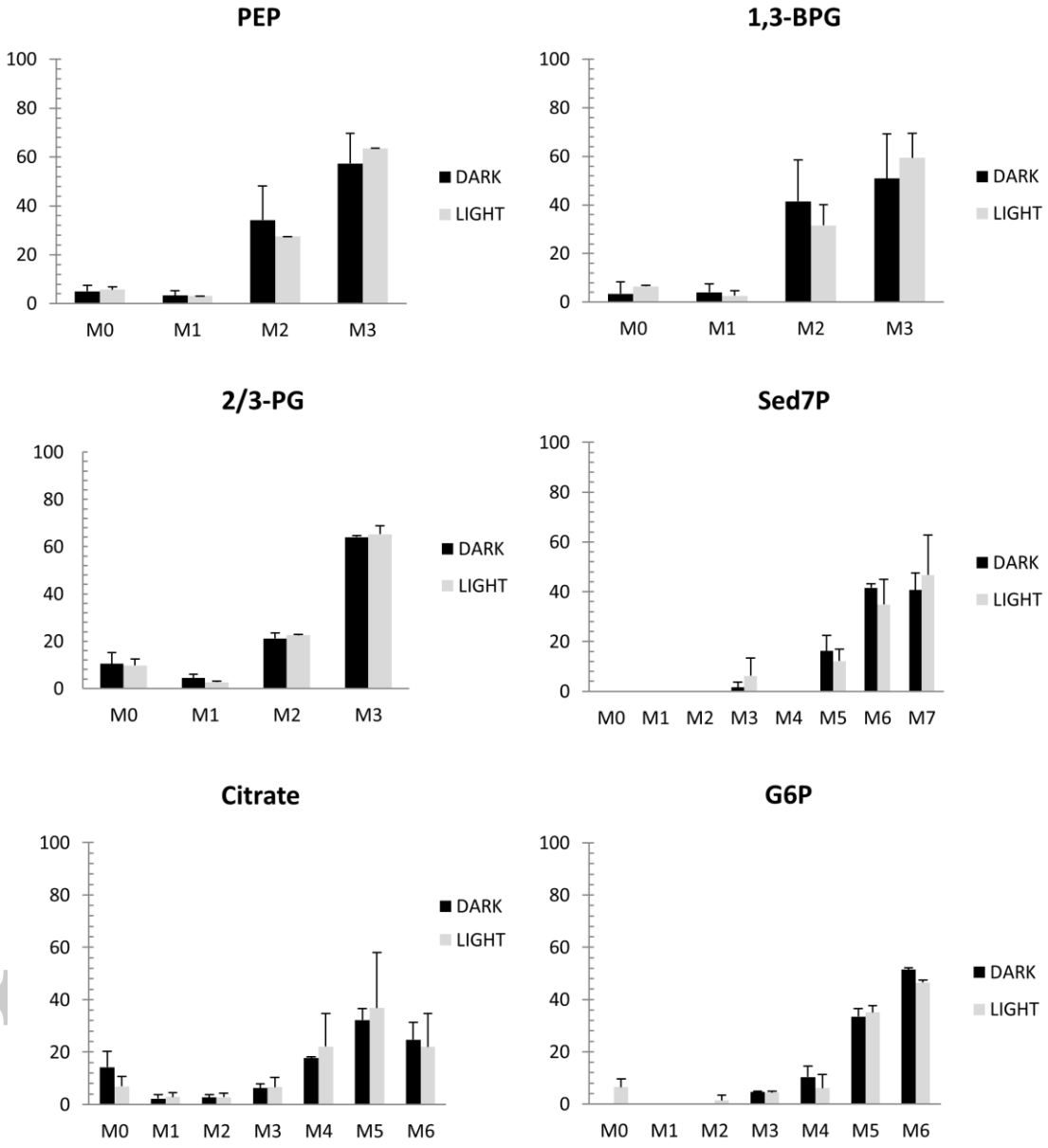

799

800 EMI_13087_F3

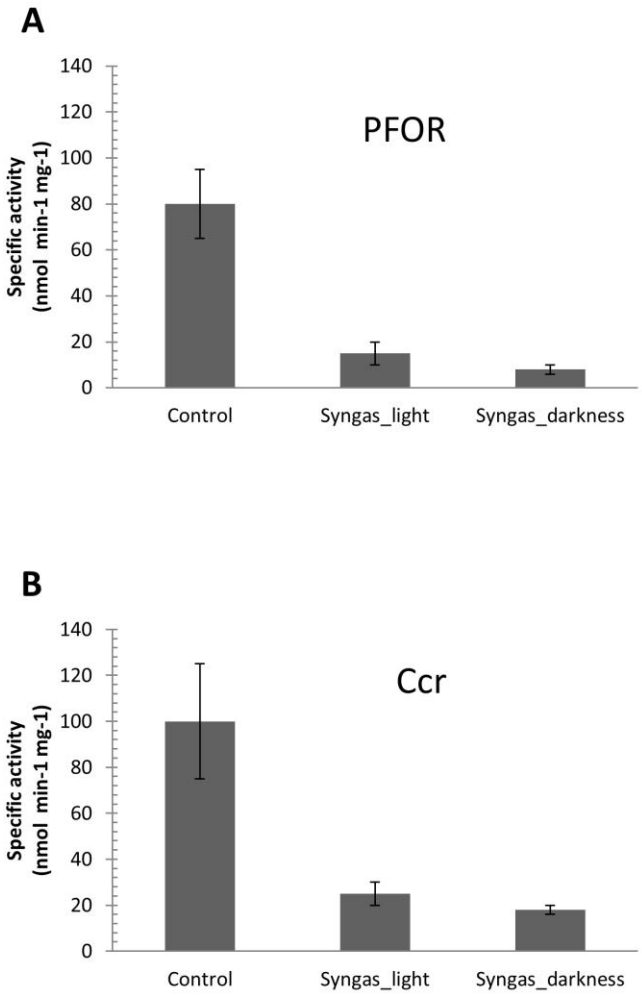

801

802 EMI_13087_F4